Decoding the anticancer activity of VO-clioquinol compound: the mechanism of action and cell death pathways in human osteosarcoma cells†

Ignacio E. León,[ab] Paula Díez, [iD][cd] Enrique J. Baran,[b] Susana B. Etcheverry*[ab] and Manuel Fuentes [iD] *[cd]

Vanadium compounds were studied in recent years by considering them as a representative of a new class of non-platinum metal anticancer drugs. However, a few challenges still remain in the discovery of new molecular targets of these new metallodrugs. Studies on cell signaling pathways related to vanadium compounds have scarcely been reported and so far this information is highly critical for identifying novel targets that play a key role in the antitumor actions of vanadium complexes. This research deals with the alterations in the intracellular signaling pathways promoted by an oxovanadium(IV) complex with the clioquinol (5-chloro-7-iodo-8-quinolinol), VO(CQ)$_2$, on a human osteosarcoma cell line (MG-63). Herein are reported, for the first time, the antitumor properties of VO(CQ)$_2$ and the relative abundance of 224 proteins (which are involved in most of the common intracellular pathways) to identify novel targets of the studied complex. Besides, full-length human recombinant AKT1 kinase was produced by using an IVTT system to evaluate the variation of relative tyrosin-phosphorylation levels caused by this compound. The results of the differential protein expression levels reveal several up-regulated proteins such as CASP3, CASP6, CASP7, CASP10, CASP11, Bcl-x, DAPK and down-regulated ones, such as PKB/AKT, DIABLO, among others. Moreover, cell signaling pathways involved in several altered pathways related to the PKC and AP2 family have been identified in both treatments (2.5 and 10 μM) suggesting the crucial antitumoral role of VO(CQ)$_2$. Finally, it has been demonstrated that this compound (10 μM, 6 h) triggers a decrease of 2-fold in *in situ* AKT1 expression.

Significance to metallomics

Understanding how vanadium compounds perform their role as anticancer agents is really important in the field of metallodrugs. While many mechanisms of action for vanadium compounds are known and have been characterized (ROS generation, cell cycle arrest, tyrosine phosphatase inhibition, and ERK1 and ERK2 activation), the present work decodes the function of many proteins (BCL10, BCL-X, CASP3, FAK and AKT1, among others) involved in the antitumor effects of vanadium compounds against human osteosarcoma.

Introduction

Metal-based drugs have a wide spectrum of pharmacological activities against different pathologies, including neurodegenerative diseases, diabetes, and cancer. The capability of metallodrugs as cancer therapeutic agents has been known since the 16th century.[1]

Cisplatin, carboplatin, and oxaliplatin are the most important and successful metal-based drugs in the clinic.[2] However, a few challenges still remain for their application (such as lack of specificity, poor absorption, or chemoresistance, among others). In this regard, medicinal inorganic chemistry is focused on the development of several approaches to overcome these difficulties, which include the design and synthesis of new metallodrugs that have different structural features.[3,4]

In this regard, vanadium compounds have recently emerged as non-platinum antitumor agents[5] showing promising anticancer effects on different types of solid tumors.[6–8]

[a] Chair of Patologic Biochemistry, Exact School Sciences, National University of La Plata, 47 y 115, 1900 La Plata, Argentina. E-mail: etcheverry@biol.unlp.edu.ar
[b] Inorganic Chemistry Center (CEQUINOR, CONICET), Exact School Sciences, National University of La Plata, 47 y 115, 1900 La Plata, Argentina
[c] Cancer Research Center (IBMCC/CSIC/USAL/IBSAL), University of Salamanca-CSIC, IBSAL, Department of Medicine, General Cytometry Service-Nucleus, Campus Miguel de Unamuno S/N, 37007 Salamanca, Spain. E-mail: mfuentes@usal.es; Fax: +34 923294743; Tel: +34 923294811
[d] Proteomics Unit, Cancer Research Center, IBSAL, University of Salamanca-CSIC, Campus Miguel de Unamuno S/N, 37007 Salamanca, Spain
† Electronic supplementary information (ESI) available. See DOI: 10.1039/c7mt00068e

The role of vanadium in the regulation of cell signaling pathways makes it a potential therapeutic agent, which can be used in the treatment of several diseases. Nevertheless, the study of activation pathways targeted by vanadium compounds have scarcely been reported in the literature, and so far, the data for the discovery of novel intracellular targets in cancer have not been completely examined. In this regard Tiago and collaborators described the importance of MAPK and PI-3K-Ras-Erk pathways on the anti-mineralogenic properties of vanadate in a fish chondrocyte cell line.[9,10]

Our recently reported results demonstrated that vanadium compounds increase the cytotoxicity levels, induce cell cycle arrest and apoptosis in human osteosarcoma cells involving AKT and FAK cell signaling pathways.[11,12] In this context, there is great interest in deciphering the targets of novel vanadium compounds affecting the cell signaling pathways related to the anticancer activity.

In the last few years, the use of protein microarrays has appeared to be a high-throughput method to provide a suitable tool for the discovery of new molecular drug targets.[13] Despite the progress in the protein microarray area, a few challenges still remain. Hence, in order to overcome these challenges, a complementary method named NAPPA (Nucleic Acid Programmable Protein Arrays) has been developed.[14] Full-length human recombinant proteins expressed *in situ* have been successfully applied for the study of protein–protein and protein–drug interactions.[15]

Here, it is proposed to identify novel targets of vanadium by using both protein array approaches (relative abundance based antibody arrays and *in situ* protein arrays). This research deals with the effects of intracellular signaling of an oxovanadium(IV) complex with the clioquinol (5-chloro-7-iodo-8-quinolinol), VO(CQ)$_2$, on a human osteosarcoma cell line (MG-63). We have investigated and reported for the first time the effect of VO(CQ)$_2$ on the relative abundance protein patterns of 224 proteins involved in most common intracellular signaling pathways and the relationship with the mechanism of cell death. In addition, full-length human recombinant AKT1 kinase has been produced *in situ* using rabbit reticulocyte lysate (RRL) *in vitro* protein expression systems; then, the protein expression levels and the inhibition of tyrosine phosphorylation sites induced by VO(CQ)$_2$ were explored.

Experimental section

Materials

Tissue culture materials were purchased from Corning (Princeton, NJ, USA), Panorama Cell Signalling Kit and RPMI 1640 (Sigma Chemical Co. St Louis, MO, USA), trypsin and fetal bovine serum (FBS) from Gibco (Gaithersburg, MD, USA), RC DC Protein Assay Kit from Bio-Rad, Protein-G-agarose beads, Cy3 and Cy5 from (GE Healthcare, CA, USA, Purefield™ Plasmid Miniprep System from (Promega, Wisconsin, USA)), mouse antibody anti-phosphotyrosine from (Millipore, MA, USA), rabbit polyclonal anti-GST from GE Healthcare, monoclonal anti-GST from Cell

Signaling, anti-mouse-HRP from (Jackson ImmunoResearch Laboratories, West Grove, PA).

The MG-63 cell line was purchased from ATCC.

Methods

Synthesis and identification of VO(CQ)$_2$

VO(CQ)$_2$ was synthesized according to previously reported results.[16] Briefly, clioquinol (0.61 g) was dissolved in 150 mL of warm ethanol. To this solution, 0.35 g of VOSO$_4$·5H$_2$O mixed in 10 mL of hot ethanol was added dropwise. The solution became dark and the complex precipitated after stirring for a short while. After digestion for a short while over a water bath, it was filtered, washed with absolute ethanol and dried for 3 days at 60 °C.

Anal. calc. for C$_{18}$H$_8$N$_2$O$_3$Cl$_2$I$_2$V C 31.91; H 1.18; N 4.14; V 7.54; exp. C 31.80; H 1.27; N 4.26; V 7.66. The identification of the complex was done by FTIR.

Preparation of VO(CQ)$_2$ solutions

Fresh stock solutions of the complex were prepared in DMSO at 20 mM and diluted according to the concentrations indicated in the legends of the figures. We used 0.5% as the maximum DMSO concentration in order to avoid the toxic effects of this solvent on the cells.

Stability of the complex in solution

To test the stability of the compound under the different experimental conditions used in this work, we analyzed the UV-visible spectra of different solutions of the complex. 20 mM solutions of complex in DMSO and 0.01 mM of complex in medium RPMI (pH = 7.4) were prepared. The electronic spectra were recorded at times ranging from 0 to 6 h at room temperature and at 37 °C. The rate of decomposition of the complex was spectrophotometrically measured.

Cell culture conditions

MG-63 cells were grown in RPMI 1640 medium containing 10% FBS, 100 U mL^{-1} penicillin and 100 μg ml^{-1} streptomycin at 37 °C under a 5% CO$_2$ atmosphere. Cells were seeded in a 175 cm^2 flask and when 70–80% confluence was reached, the cells were subcultured using 4 mL of trypsin per 175 cm^2 flask. For experiments, cells were grown in a 75 cm^2 flask for 24 h at 37 °C. Then, the monolayer was incubated with different concentrations (25 and 100 μM) of the complex.

Measurement of the exposure of phosphatidylserine (PS) by annexin V-FITC/PI staining

Cells in early and late stages of apoptosis were detected by annexin V-FITC and propidium iodide (PI) staining. Thus, cells were washed with PBS and adjusted to a concentration of 1 × 10^6 cell per mL in 1 mL binding buffer (0.01 M HEPES, pH 7.4; 0.14 M NaCl; 2.5 mM CaCl$_2$). To 100 μL of cell suspension, 2.5 μL of annexin V-FITC were added and incubated for 15 min at room temperature. Finally, 2 μL PI (250 mg mL^{-1}) were added prior to analysis. Cells were analyzed using a flow

cytometer CyAn™ ADP (Beckman Coulter, USA) and Summit v4.3 software.

Mitochondrial membrane potential (MMP)

The cells cultured in 24-well plates were washed with PBS and incubated with 5 μg ml^{-1} rhodamine 123 for 30 min at 37 °C. After further washing, the cells were incubated with DMEM for 30 min. The changes in MMP were analyzed using a flow cytometer CyAn™ ADP (Beckman Coulter, USA) and Summit v4.3 software.

Subcellular protein fractionation and dye-labeling

Cytoplasmic proteins were isolated by using a sub-fractionation protocol. The cells were harvested and washed three times with PBS. Then, three portions of lysis buffer were added (5 mM HEPES, 10 mM MgCl$_2$, 140 mM NaCl, 0.1% (v/v) Tween 20 at pH 8.0, 1% (v/v) protease inhibitor mix). Briefly, lysed cells were centrifuged for 15 min at 15 000g at 4 °C. After that, the supernatant was collected and 10% (w/v) octyl-β-$_D$-glucopyranoside was added followed by sonication (3 times with 3 second bursts). Samples were preserved on ice for 30 min and then centrifuged, yielding the cytoplasmic fraction. Immediately after IgG depletion (by using protein-G-agarose beads), purified proteins were quantified by Lowry assay following the manufacturer's instructions. Then, cytoplasmic proteins were conjugated with Cy3 or Cy5 at a dye/protein ratio >2 following the manufacturer's recommendations.

Antibody microarray assays

The functional proteomic analysis was performed by using the Panorama Cell Signaling Kit following the manufacturer's instructions. The antibody microarray consists of 224 human monoclonal antibodies targeting proteins involved in intracellular signaling pathways, spotted in duplicate onto a nitrocellulose-coated slide. Equal amounts of fluorescently labeled proteins of osteosarcoma cells from basal condition (control) and from treatments with vanadium complex (each with a different dye) were incubated with the microarray slide at RT for 1 h on an orbital shaker. For optimal and robust characterization of the differences in relative protein abundance under all the tested conditions, and according to the manufacturer, only proteins that presented a Cy5/Cy3 ratio ≥2 (up) and a ratio Cy5/Cy3 ≤0.5 (down) have been taken into consideration for the identification of altered intracellular pathways.

Antibody microarray data analysis

Microarrays were scanned using Scanner GenePix 4000B (Axon, USA) using Cy3 and Cy5 settings. The images were analyzed using GenePix Pro 4.0 software (Axon, USA).

Firstly, background correction for each spot was locally obtained by applying standardized settings of GenePix software. Then, the mean value of the set of negative control spots in each fluorescence channel was subtracted from the individual spot values. Before statistical analysis (MultiExperiment Viewer (MeV) clustering and Significance Analysis of Microarrays (SAM)), the raw intensity data for each slide were normalized by reference (housekeeping) proteins. The fluorescence intensity obtained for each protein in the array was divided by the fluorescence intensity obtained for a highly expressed reference protein. We performed a Z-score estimation for the housekeeping proteins in the array and selected those with a high value (>2) for the normalization.

In all cases, the mean of the protein replicates was calculated to obtain a single value per protein/assay.[17]

Functional annotation of down-/up-regulated expressed proteins

Altered-expression proteins were selected by computing a relation between each condition (control $vs.$ vanadium treatment) after applying the normalization strategy described above. Significance was assigned to proteins whose ratio was greater than or equal to 2.0 or less than or equal to 0.5.

The functional annotation of the selected proteins was analyzed using the GeneCodis tool including gene ontology (GO) annotations and Circos software.

Self-assembled protein arrays in the multi-well format (NAPPA-ELISA)

The list of candidate kinases selected for targeted screening was built on the basis of the Panorama Cell Signaling Kit results. The cDNA (encoding corresponding full-length human proteins) employed in the NAPPA-ELISA is AKT1.

cDNA preparation

Escherichia coli bearing a total of 2 sequence-verified full-length human genes in pANT7_cGST were obtained from the Center for Personalized Diagnostics at the Arizona State University and are publicly available (www.dnasu.org). Bacteria were grown for 24 h at 37 °C in 100 mL of Luria–Bertani medium supplemented with ampicillin for cGST clones. The cells were pelleted and their plasmid DNA was purified using the Purefield™ Plasmid Miniprep System according to the manufacturer's instructions.

In situ protein expression

The *in vitro* transcription and translation steps were performed as previously described by Manzano-Román *et al.*[18] The transcription/translation lysate mix was added into the tubes. The tubes were incubated for 1.5 h at 30 °C for protein expression and capture using an anti-GST polyclonal rabbit antibody.

NAPPA-ELISA assay

A GST fused to the AKT1 full-length human gene was expressed *in vitro* using the rabbit reticulocyte lysate, as previously described.[18,19]

The FAK and AKT1 proteins were then applied onto anti-GST-coated 96-well plates. The plates were washed with 0.02% PBS-Tween and blocked with PBS–Tween with 5% milk overnight at 4 °C. After washing, the plate was incubated with the 1:1000 (v/v) diluted anti-GST and anti-phosphotyrosine mouse antibodies. The presence of the specific protein was detected by incubation with the HRP-linked anti-mouse secondary antibody diluted 1:1000 (v/v) in assay buffer. A tetramethylbenzidine substrate was then added and

the reaction was stopped. The 450 nm signals were read and the absorbances were subjected to t-test analysis to determine the significance of any variation in the antibody levels between the samples.

Results and discussion

Synthesis, characterization and stability studies of VO(CQ)$_2$

VO(CQ)$_2$ (Fig. 1A) was synthesized as previously described by Gonzáles Baró and Baran[16] (see the Experimental section). The final product was characterized by FTIR, with the main vibrations being fully comparable with the organic moiety, allowing an accurate identification.

Since DMSO has been used as a co-solvent in biological systems, we explored the stability of the VO(CQ)$_2$ complex in DMSO and RPMI solutions (pH = 7.4) using UV-vis spectroscopy. In the electronic absorption spectrum of VO(CQ)$_2$ (0.02 M in DMSO solution) one d–d transition was observed at 782 ($\varepsilon = 51$ M^{-1} cm^{-1}). Upon monitoring this solution with time (0.25, 0.5, 1, 2, 3 and 6 h), no changes were observed in the UV-vis signals, and the integrity of the complex in DMSO was intact within the time-frame of the biological experiments (see Fig. 1B). Besides, in the electronic absorption spectrum of VO(CQ)$_2$ (0.00001 M in RPMI solution) one charge transfer band was observed at 295 nm ($\varepsilon = 27\,000$ M^{-1} cm^{-1}) and upon monitoring this solution no changes were observed.

These results suggest that the compound does not undergo oxidation and is stable over time.

Cytotoxic activity and apoptosis induced by VO(CQ)$_2$ in human osteosarcoma MG-63 cells

VO(CQ)$_2$ caused a concentration-dependent inhibition of cell viability in human osteosarcoma MG-63 cells. The anti-proliferative action of the complex is much stronger as a consequence of a cooperative/synergy effect of the free clioquinol and the vanadyl cation, demonstrating the improvement of the antitumoral action through the complexation of the ligand with vanadyl(IV). This is also evident from the IC$_{50}$ values in MG-63

cells: VO(CQ)$_2$ *ca.* 7 μM while for clioquinol this value is 59 μM and for VO$^{(+2)}$ the IC$_{50}$ value is >100 μM (see Fig. 2A).

Mitochondria are one of the most important organelles that can regulate cellular apoptosis.[20] To elucidate whether VO(CQ)$_2$ induces cytotoxicity in human osteoblasts by alterations of mitochondrial functions, we evaluated the Mitochondria Membrane Potential (MMP) in MG-63 cells under control conditions and in the presence of different concentrations (1 and 2.5 μM) of the compound.

After 24 h of incubation, as can be seen in Fig. 2B and Fig. S1 (ESI†), the fluorescence intensity of rhodamine 123 shifted to the left, indicating the dissipation of MMP as the dose of the complex increased. The fractions of cells that displayed low fluorescence intensities were 20, 27 and 47% for 0, 1 and 2.5 μM of VO(CQ)$_2$, respectively. The results suggest that the effect of the compound on MMP is, at least partly, one of the principal mechanisms of action involved in the antitumoral actions of VO(CQ)$_2$. In order to confirm the MMP obtained results and to obtain deeper insight into the apoptosis induced by VO(CQ)$_2$, we tested four concentrations of the complex (1, 2.5, 5, and 10) and two incubation times (6 and 24 h). Table 1, Fig. 2(C and D) and 3 display the quantification of the early and late stages of apoptosis obtained by flow cytometry in MG-63 cells. As can be seen, after 6 h of incubation the control cultures showed 0.47% of early apoptotic cells (annexin V positive) and 2.5% of late apoptotic cells (annexin V positive/ propidium iodide (PI) positive). These results changed with the treatment showing an increase in the early apoptotic cellular fraction (8.1%) and the late apoptotic cells (9%).

After 24 h of incubation, VO(CQ)$_2$ resulted in approximately 6% of early apoptotic cells at 5 μM (*vs.* 1% of basal conditions) whilst this compound increased 17, 27 and 42% cells of late apoptotic features at 1, 2.5 and 5 μM, respectively (*vs.* 6% of control).

These results are in accordance with the viability assays, confirming that the deleterious action of VO(CQ)$_2$ is dependent on its concentration and time in the MG-63 cell line.

On the other hand, the results indicate that VO(CQ)$_2$ has greater antitumor actions in human osteosarcoma cells than in non-transformed mouse fibroblasts (L929).
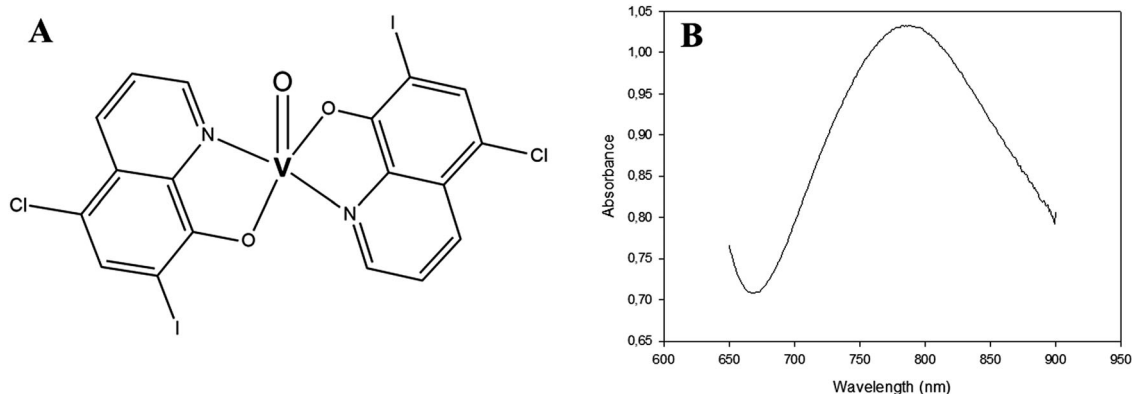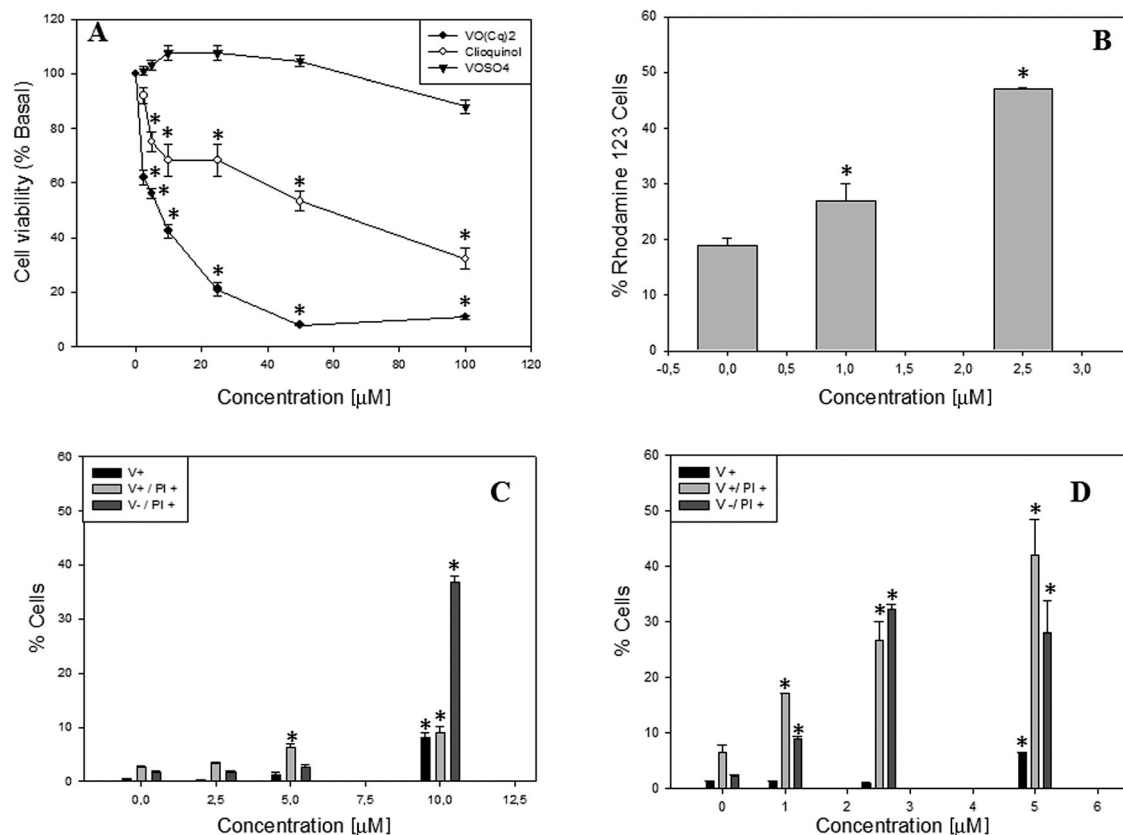

Fig. 1 Vanadium complex structure. (A) Chemical proposed structure of the oxovanadium(IV)−clioquinol complex; (B) UV-vis spectra of VO(CQ)$_2$ (0.02 M) in DMSO solution.

Fig. 2 Effect of VO(CQ)$_2$ on cell viability and apoptosis (B–D). (A) Cell viability test: MG-63 cells were treated with VO(CQ)$_2$ at 0–100 μM (1, 2.5, 5, 10, 25, 50 and 100 μM) at 37 °C for 24 h. (B) Mitochondrial membrane potential (MMP) assay: MG-63 cells were treated with VO(CQ)$_2$ at 0, 1 and 2.5 μM at 37 °C for 24 h. (C and D) Apoptosis studies: MG-63 cells were treated with VO(CQ)$_2$ at 0, 1, 2.5 and 5 μM at 37 °C for 6 and 24 h. The cell viability test was assessed by MTT and the apoptosis studies by flow cytometry using rhodamine 123 (B) and annexin V–fluorescein isothiocyanate (FITC)/propidium iodide (PI) staining (C and D).

Table 1 Percentage of apoptotic cells treated with VO(CQ)$_2$. The results are expressed as the mean ± the standard error of the mean of three independent experiments ($n = 9$)

	Annexin V+/PI−		Annexin V+/PI+	
VO(CQ)$_2$	6 h	12 h	6 h	12 h
0 μM	0.47	1.13	2.50	6.50
1 μM	ND	1.25	ND	17.50*
2.5 μM	0.40	0.97	3.25	26.80*
5 μM	1.20	6.30*	6.15*	42.00*
10 μM	8.10*	ND	9.00*	ND

PI, propidium iodide.* significant differences *vs.* the control ($p < 0.01$).

As a whole, these results demonstrate that VO(CQ)$_2$ is a potentially very good candidate for further evaluation of its molecular targets since it is less toxic to the normal phenotype cells (L929) and is highly deleterious for the human osteosarcoma cells.

Decrypting altered cell signaling pathways by VO(CQ)$_2$ treatment in human osteosarcoma MG-63 cells

Based on the biological results previously described, and in order to identify the relative differences in protein patterns, a time and concentration course treatment in MG-63 cells with

VO(CQ)$_2$ was achieved with abundance-based protein arrays as described in the Experimental section. According to reported data about VO(CQ)$_2$, several comparison studies were performed with soluble proteins (*i.e.*, cytoplasmatic, nuclear, among others) from control conditions and different treatments with VO(CQ)$_2$ (2.5 μM 6 h and 10 μM 6 h). This experimental proposal allows decoding of altered cell signaling pathways by the effect of VO(CQ)$_2$ by studying global differential protein expression profiles and the potential correlation with the anticancer activity of this metallodrug in human osteosarcoma cells.

Table 2 shows that after 6 h and 2.5 μM VO(CQ)$_2$ treatment (condition 1), forty-nine up-regulated proteins and eleven down-regulated proteins were detected (see S3, ESI†), while for condition 2, the vanadium compound only up-regulated twenty proteins (see S4, ESI†). Taken together, these results demonstrate the presence of significant differences in protein expression profiles as a consequence of the expected targeted effect of this metallo-drug in several intracellular signaling pathways. The main proteins identified within differential expression profiles are grouped and discussed below in canonical signaling pathways: (1) apoptosis, (2) cell cycle, (3) cell stress and (4) signalling transduction.

Fig. 4 shows a summary of altered relative protein abundance detected in each treatment with VO(CQ)$_2$. As it can be seen in the
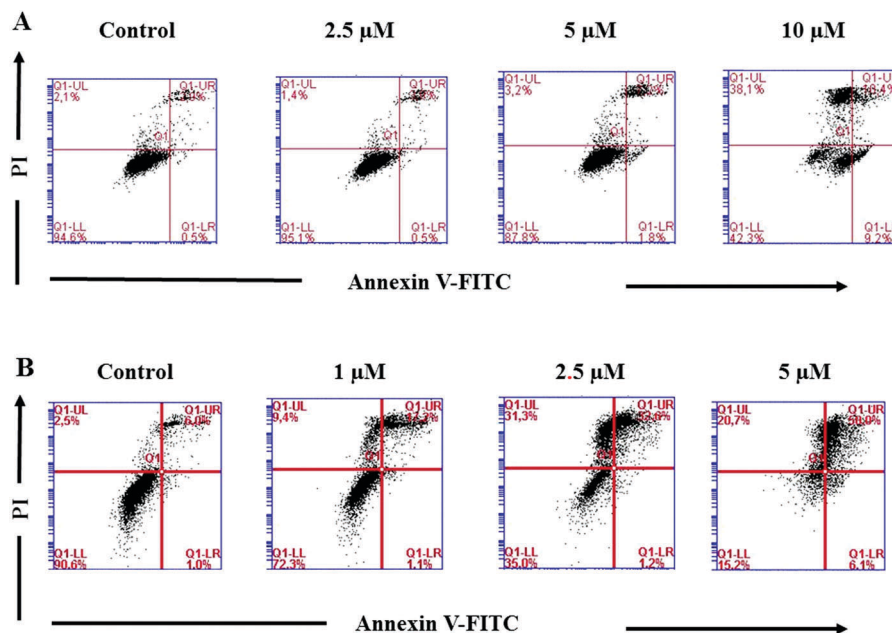
Fig. 3 Apoptosis studies after 6 h (A) and 24 h (B) of incubation. The plots are representative of three independent experiments. The numbers in the Q1-LR and Q1-UR quadrants indicate the proportions of cells that are annexin V positive/PI negative and annexin V positive/PI positive, respectively.

Table 2 Global effect of VO(CQ)$_2$ in relative protein abundance after 6 h treatment

Condition	Concentration (μM)	No. up-regulated proteins	No. down-regulated proteins
1	2.5	49	11
2	10.0	20	0

Fig. 4A (2.5 μM VO(CQ)$_2$), the complex induced the increase of relative levels of antiapoptotic proteins (Bcl-x) and pro-apoptotic proteins (Bcl-10, CASP6, CASP7, CASP10 and CASP11). Besides, this compound shows an effect on up-regulation of the level of phosphatidylserine receptor (early apoptosis biomarker) and on the DAP-kinase levels (a late apoptosis biomarker) in concordance with previous results described above. Moreover, low abundance protein levels of active CASP3, PAR4 and SMAC/DIABLO, all proteins with a pro-apoptotic function, have been reported. The down-regulation levels of these important proteins involved in the apoptosis process may be an alternative for tumor escape and chemoresistance. This down-regulation may be mediated by Bcl-x, which acts as an anti-apoptotic protein by preventing the release of mitochondrial contents (cytochrome c). These actions lead to caspase activation and induce apoptosis.

Additionally, the Cy5/Cy3 ratio of Bcl-x is higher for condition 1 than condition 2 (2.89 vs. 2.18). This effect of the complex concentration may explain the up-regulation level of active CASP3 for condition 2 (see Fig. 4B) and its cross-regulation with Bcl-x. This fact has been previously demonstrated by many scientific reports showing a close relationship between Bcl-x and pro-apoptosis proteins.[21,22]

Moreover, VO(CQ)$_2$ seems to induce the up-regulation of several proteins involved in the cell cycle regulation, such as

c-Myc, E2F1, cyclin D3, p21Waf-1, SMAD4, Ap-1/cjun, ATF2, HADC4, and PCAF, among others, suggesting the key role of these transcription factors in cell cycle progress and apoptosis. Besides, for condition 1, several cytoskeleton-related proteins (cytokeratin family, myosin…) were detected as up-regulated. On the other hand, PKB/AKT pathways are down-regulated suggesting the important role of these pathways in the anti-cancer activity of VO(CQ)$_2$. In this way, several research reports showed the relevant relationship between blocked AKT pathways and apoptosis inhibition.[23,24] In addition, the interaction between vanadium compounds with anti-diabetic actions and the AKT cell signaling pathway has been reported.[25,26]

Other important findings for condition 2 are related to HSP90 and Nedd 8, which appeared to be up-regulated. HSP90 and Nedd 8 stabilize a number of proteins required for tumor growth, which are involved in the cell stress response suggesting that the osteosarcoma tumor may use these proteins for an alternative way toward drug chemotherapy.

Ten up-regulated proteins were identified to be common between conditions 1 and 2 (Fig. 4). In both cases, there was an enrichment in FAK (Tyr^{577}), HSP90, PKCb, PKCg, AP2beta, AP2gamma, AP2alpha, DOPA decarboxylase and glutamate receptor NMDAR 2a.

The levels of PKCb and PKCg are higher for condition 2 than condition 1, suggesting the importance of these kinases in the anticancer activity of VO(CQ)$_2$ (see Fig. 4). In this regard, Mehdi and co-workers established that PKC protein is required to stimulate PKB/AKT phosphorylation in response to the anti-diabetic actions of vanadium(IV) oxo-bis(maltolate) (BMOV) in HepG2 cells.[27] In the same way, relative levels of PKC were up-regulated, which could be linked to restoring the proteasome activity and abrogating osteosarcoma cellular differentiation.[28]
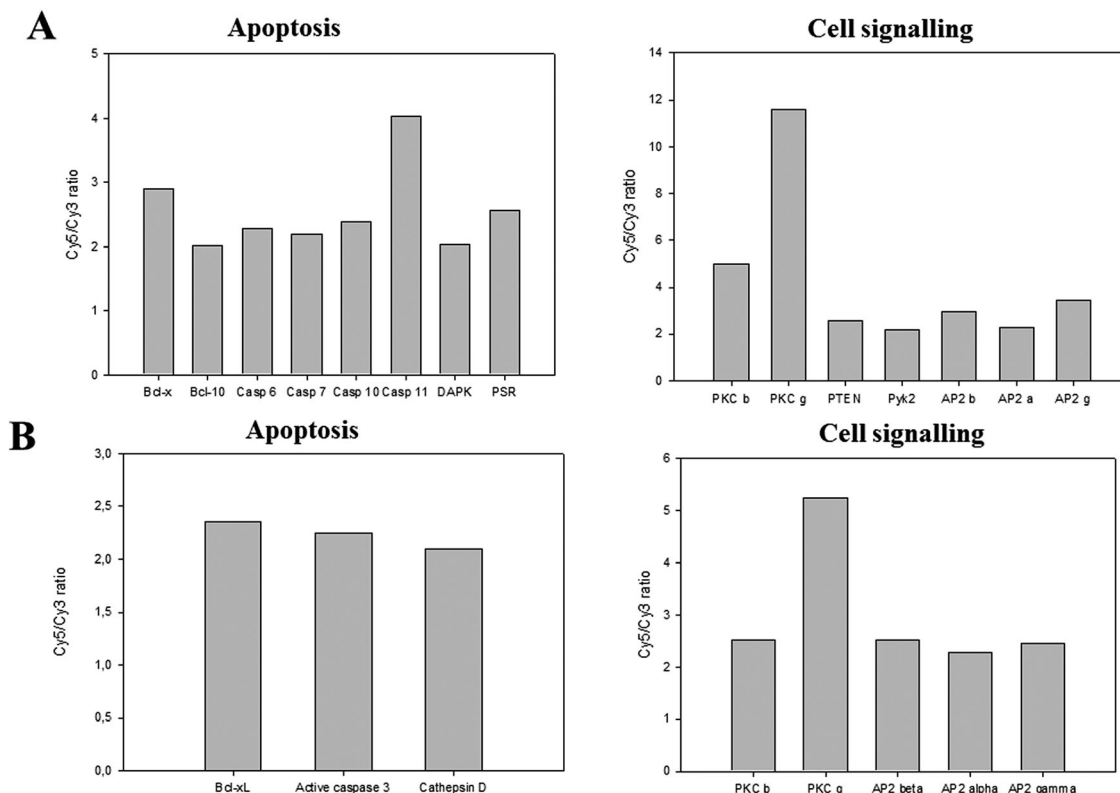
Fig. 4   Main altered proteins detected in each group of treatment. (A) Values of the Cy5/Cy3 ratio for the treatment with 2.5 μM of VO(CQ)$_2$. (B) Values of the Cy5/Cy3 ratio for the treatment with 10 μM of VO(CQ)$_2$.

For focal adhesion kinase (FAK), the results showed that the compound up-regulated the site of phosphorylation Tyr[577] (see Data S3 and S4, ESI†). The Tyr[577] site of tyrosine phosphorylation is one of the most important regulatory sites of FAK. In this way, Tyr[577] produce FAK bis-phosphorylated at Tyr[576] and Tyr[577].[29] The level of Tyr[577] is higher for condition 1 than for condition 2 (see Data S3 and S4, ESI†), suggesting the importance of this site of phosphorylation in the response of tumor against chemotherapeutic drug actions.

FAK, also known as protein kinase 2 (PTK2), is a protein tyrosine kinase that controls motility, proliferation, and survival in several types of solid tumors. Interestingly, FAK is well-characterized as over-expressed and activated in several advanced-stage solid cancers and it promotes tumor progression and metastasis.[30] Consequently, FAK has become a potential prognostic marker and antitumor molecular target.[31] In addition, FAK and EGFR also induce cooperative signals that suppress apoptosis and enhance cell survival in breast cancer cells through activation of the ERK and AKT pathways.[32]

On the other hand, the AP2 family (alpha, beta, and gamma) was up-regulated in both treatments (conditions 1 and 2). These results suggest that this family of transcription factors may be involved in the anticancer activity of VO(CQ)$_2$. In this context, several scientific reports showed a direct correlation in the over-expression of the AP2 family and the inhibition of cancer cell growth in different types of cancers, such as liver, breast, and colon.[33–35] Our results showed the up-regulation of

AP2 family proteins and the universal cell cycle inhibitor (p21WAF1), suggesting a strong correlation between both proteins. Similar results were described by Zeng *et al.* for HepG2 human hepatoblastoma and SW480 human colon adenocarcinoma.[35]

In order to get a deeper insight into the biological context, all the up/down differentially expressed proteins in different treatments were subjected to functional characterization using the bioinformatics software DAVID 6.7 (S5–S7, ESI†).

Identification of potential novel targets by determination of differential expression profiles

We set out to characterize the potential molecular targets and the related pathways involved in the anticancer actions of VO(CQ)$_2$ against human osteosarcoma cells. To perform cell signaling pathway analysis, the down- and up-regulated proteins identified in each group of treatment have been included in the analysis. In Fig. 5, the PKC family (PKCb, PKCg), FAK (Tyr[577]), HSP90, AP2 family (beta, gamma, and alpha) and MAPK1 were common in all the treatments suggesting the significant role of these proteins associated with the anticancer activity of VO(CQ)$_2$.

In addition, as it can be seen in Fig. 6A, the role of these proteins in cancer cell signaling pathways confirmed the complexity interaction network of the different proteins with differential functions related to the anticancer effects of VO(CQ)$_2$. Moreover, PKC activates PI3K and PKB/AKT increasing gene transcription levels involved in evading apoptosis, proliferation and sustained angiogenesis, such as Bcl-xL. On the other hand,
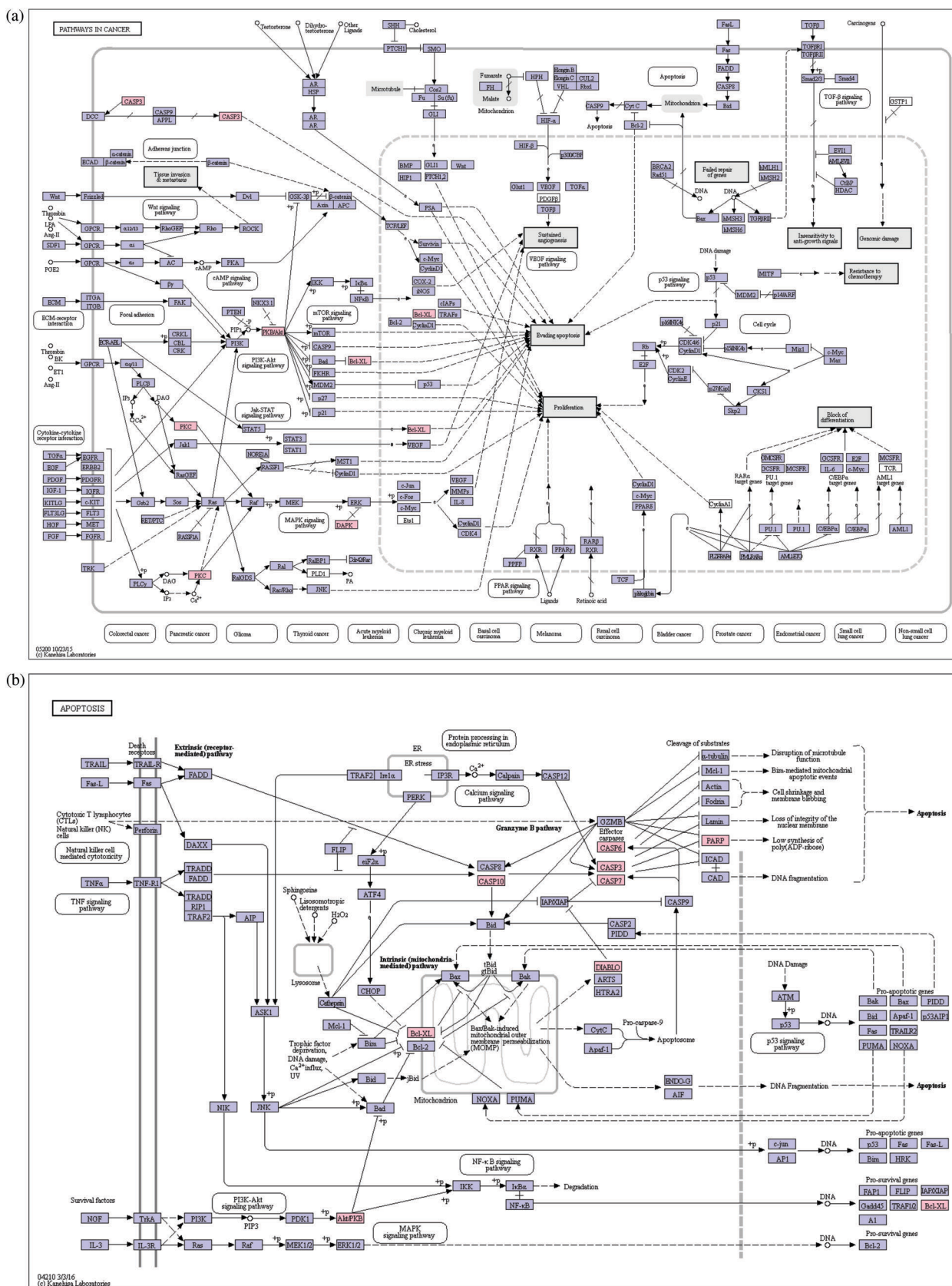
Fig. 5 Circos representation. The outer circos data track shows the differential protein pathways in each group of the study. The AP2, PKC, FAK, and MAPK1 were common in all the treatments (green, light green, red and blue, respectively). T1 (2.5 μM) and T2 (10 μM).

CASP3 and DAPK (related to the inhibition of the ERK pathway) convey to apoptosis. Moreover, Fig. 6B shows the important role of CASP10 that activates CASP3, CASP6, and CASP7 that exert an inhibition on PARP, lamin, fodrin, and actin. These proteins control the regulation of actin cytoskeleton through activation of the actin polymerization and actin filament turnover; therefore, the loss of integrity of the cell membrane and the membrane bleb formation trigger programmed cell death. Besides, PKB/AKT phosphorylate Bad and inhibit the Bcl2 and Bcl-XL (anti-apoptotic functions) whilst cathepsin exerts a direct inhibition of Bcl-xL functions.

Functional validation assay by IVTT *in situ* protein expression of targeted VO(CQ)$_2$ kinases

The effect of VO(CQ)$_2$ on kinases has been validated by functional screening using IVTT recombinant human kinase assays.

The human full-length recombinant AKT1 kinase (GST-tagged in COOH terminus) was expressed by using a cell-free protein IVTT expression system. Hence, AKT1 kinase was selected based on Panorama array results and due to its promising therapeutic applications. In both cases, the full-length IVTT expressed recombinant protein was detected by anti-GST mouse antibody. The results show that the presence of VO(CQ)$_2$ does not affect the IVTT protein expression.

In order to study the pattern of tyrosine phosphorylation sites induced by VO(CQ)$_2$ in AKT1 kinase, we evaluated the phospho-tyrosine/GST signal ratio.

The values for the Tyr/GST ratio are 0.38 (control), 0.24* (2.5 μM) and 0.19* (10 μM), respectively. These results showed that VO(CQ)$_2$ generated a reduction in the Tyr/GST ratio suggesting that the complex diminished the level of tyrosine phosphorylation of AKT kinase with statistical significance (*$p < 0.01$). These results

(a)

(b)

Fig. 6 Cancer cell signaling pathways induced by VO(CQ)$_2$. The cell signaling pathway graphic shows the role of different proteins down-/up-regulated by VO(CQ)$_2$ in cancer pathways (CASP3, DAPK, BCL-xL, PKB, PKC) (a) and apoptosis (CASP3, CASP6, CASP7, CASP10, PARP, DIABLO, cathepsin, BCL-xL) (b).
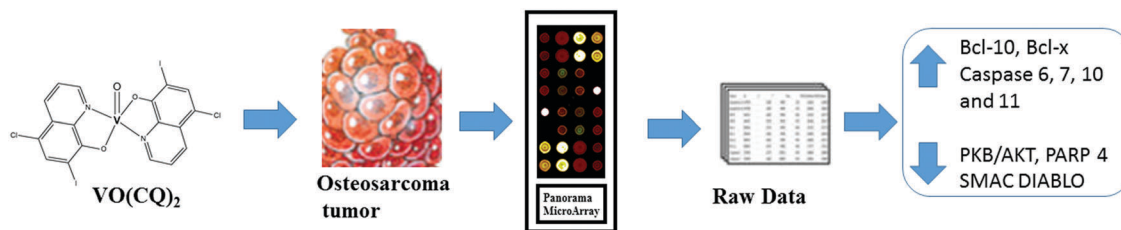
Fig. 7   Results overview. A brief scheme of antitumor effects of VO(CQ)$_2$ on osteosarcoma cells.

correlate with the data obtained in the antibody array study, in which we could establish that the complex down-regulated the PKB/AKT pathways signifying the important role of this pathway in the anticancer activity of VO(CQ)$_2$.

Our results show that VO(CQ)$_2$ selectively inhibits the phosphorylation of AKT1 kinase, whereby the complex may act as a down-regulator of AKT1 cell signaling (see Fig. 6B).

Conclusion

New oxovanadium complexes with potential antitumor properties currently require more intensive exploration since information obtained from the *in vitro* studies may allow vanadium drugs to enter the preclinical *in vivo* phase. On this basis, we have thoroughly investigated the novel targets of the oxovanadium(IV)– clioquinol compound by using antibody arrays platforms and *in situ* protein arrays.

We have investigated and reported herein for the first time the effects of VO(CQ)$_2$ on intracellular signaling in a human osteosarcoma cell line (MG-63) and the relationship with the pro-apoptotic activity of this compound. Besides, we have studied the protein expression levels and the inhibition of tyrosine phosphorylation induced by VO(CQ)$_2$. The results showed that the compound up-regulated proteins (CASP3, CASP6, CASP7, CASP10, Bcl-10, Bcl-x) and caused the down-regulation of important proteins, such as PKB/AKT, PARP, DIABLO, among others (see Fig. 7). Besides, the PKC family, FAK, HSP90, AP2 family (beta, gamma, and alpha) and MAPK1 were found to be commonly expressed in both treatments suggesting the key role of these proteins in the antitumor activity of VO(CQ)$_2$.

On the other hand, the compound reduced the Tyr/GST ratio of AKT1, demonstrating the importance of inactivation of the AKT pathway in the antitumor effects of this vanadium compound.

Taken together, these results indicate that VO(CQ)$_2$ is a promising candidate with potential anticancer activity providing new insights into the design of vanadium compounds as potential anticancer agents.

Acknowledgements

References

1   M. Frezza, S. Hindo, D. Chen, A. Davenport, S. Schmitt, D. Tomco and Q. P. Dou, *Curr. Pharm. Des.*, 2010, **16**, 1813–1825.

2   M. Apps, E. Choi and N. Wheate, *Endocr. Relat. Cancer*, 2015, **22**, R219–R233.

3   J. S. Butler and P. J. Sadler, *Curr. Opin. Chem. Biol.*, 2013, **17**, 175–188.

4   N. P. E. Barry and P. J. Sadler, *Chem. Commun. (Camb).*, 2013, **49**, 5106–5131.

5   I. E. León, J. F. Cadavid-Vargas, A. L. Di Virgilio and S. Etcheverry, *Curr. Med. Chem.*, 2017, **24**, 112–148.

6   Y. Dong, R. K. Narla, E. Sudbeck and F. M. Uckun, *J. Inorg. Biochem.*, 2000, **78**, 321–330.

7   R. K. Narla, Y. Dong, D. Klis and F. M. Uckun, *Clin. Cancer Res.*, 2001, **7**, 1094–1101.

8   I. E. León, N. Butenko, a. L. Di Virgilio, C. I. Muglia, E. J. Baran, I. Cavaco and S. B. Etcheverry, *J. Inorg. Biochem.*, 2014, **134**, 106–117.

9   D. M. Tiago, M. L. Cancela, M. Aureliano and V. Laizé, *FEBS Lett.*, 2008, **582**, 1381–1385.

10 V. Laizé, D. M. Tiago, M. Aureliano and M. L. Cancela, *Cell. Mol. Life Sci.*, 2009, **66**, 3831–3836.

11 I. E. León, P. Díez, S. B. Etcheverry and M. Fuentes, *Metallomics*, 2016, **8**, 739–749.

12 I. E. Leon, A. L. Di Virgilio, V. Porro, C. I. Muglia, L. G. Naso, P. A. M. Williams, M. Bollati-Fogolin and S. B. Etcheverry, *Dalton Trans.*, 2013, **42**, 11868–11880.

13 E. Orenes-Piñero, R. Barderas, D. Rico, J. I. Casal, D. Gonzalez-Pisano, J. Navajo, F. Algaba, J. M. Piulats and M. Sanchez-Carbayo, *J. Proteome Res.*, 2010, **9**, 164–173.

14 N. Ramachandran, J. V Raphael, E. Hainsworth, G. Demirkan, M. G. Fuentes, A. Rolfs, Y. Hu and J. LaBaer, *Nat. Methods*, 2008, **5**, 535–538.

15 J. Huang, H. Zhu, S. J. Haggarty, D. R. Spring, H. Hwang, F. Jin, M. Snyder and S. L. Schreiber, *Proc. Natl. Acad. Sci. U. S. A.*, 2004, **101**, 16594–16599.

16 A. C. Gonzalez-Baró and E. J. Baran, *Monatshefte Chemie Chem. Mon.*, 1997, **128**, 323–335.

17 P. Díez, N. Dasilva, M. González-González, S. Matarraz, J. Casado-Vela, A. Orfao and M. Fuentes, *Microarrays*, 2012, **1**, 64–83.

18 R. Manzano-Román, V. Díaz-Martín, M. González-González, S. Matarraz, A. F. Álvarez-Prado, J. LaBaer, A. Orfao, R. Pérez-Sánchez and M. Fuentes, *J. Proteome Res.*, 2012, **11**, 5972–5982.

19 F. Henjes, L. Lourido, C. Ruiz-Romero, J. Fernández-Tajes, J. M. Schwenk, M. Gonzalez-Gonzalez, F. J. Blanco, P. Nilsson and M. Fuentes, *J. Proteome Res.*, 2014, **13**, 5218–5229.

20 D. Grebenová, K. Kuzelová, K. Smetana, M. Pluskalová, H. Cajthamlová, I. Marinov, O. Fuchs, J. Soucek, P. Jarolím and Z. Hrkal, *J. Photochem. Photobiol. B.*, 2003, **69**, 71–85.

21 S. Kim, D. E. Kim, T. K. Kwon, J. Lee and J.-W. Park, *Int. J. Oncol.*, 2016, **49**, 2620–2628.

22 I. Vardaki, C. Sanchez, P. Fonseca, M. Olsson, D. Chioureas, G. Rassidakis, A. Ullén, B. Zhivotovsky, M. Björkholm and T. Panaretakis, *Blood*, 2016, **128**, 2655–2665.

23 Y. Tan, N. Huang, X. Zhang, J. Hu, S. Cheng, L. Pi and Y. Cheng, *Oncotarget*, 2016, **7**, 87100–87113.

24 W.-C. Chiu, Y.-C. Lee, Y.-H. Su, Y.-Y. Wang, C.-H. Tsai, Y.-A. Hou, C.-H. Wang, Y.-F. Huang, C.-J. Huang, S.-H. Chou, P.-W. Hsieh and S.-S. F. Yuan, *PLoS One*, 2016, **11**, e0166453.

25 J.-C. Liu, Y. Yu, G. Wang, K. Wang and X.-G. Yang, *Metallomics*, 2013, **5**, 813–820.

26 M. S. Bhuiyan and K. Fukunaga, *J. Pharmacol. Sci.*, 2009, **110**, 1–13.

27 M. Z. Mehdi, G. Vardatsikos, S. K. Pandey and A. K. Srivastava, *Biochemistry*, 2006, **45**, 11605–11615.

28 M. Fujita, S. Sugama, M. Nakai, T. Takenouchi, J. Wei, T. Urano, S. Inoue and M. Hashimoto, *J. Biol. Chem.*, 2007, **282**, 5736–5748.

29 E. Ciccimaro, J. Hevko and I. A. Blair, *Rapid Commun. Mass Spectrom.*, 2006, **20**, 3681–3692.

30 H. Yoon, J. P. Dehart, J. M. Murphy and S.-T. S. Lim, *J. Histochem. Cytochem.*, 2015, **63**, 114–128.

31 Y.-L. Tai, L.-C. Chen and T.-L. Shen, *Biomed Res. Int.*, 2015, **2015**, 690690.

32 W. Liu, D. A. Bloom, W. G. Cance, E. V Kurenova, V. M. Golubovskaya and S. N. Hochwald, *Carcinogenesis*, 2008, **29**, 1096–1107.

33 L. A. McPherson, *J. Biol. Chem.*, 2002, **277**, 45028–45033.

34 W. Huang, C. Chen, Z. Liang, J. Qiu, X. Li, X. Hu, S. Xiang, X. Ding and J. Zhang, *Int. J. Oncol.*, 2016, **48**, 1125–1134.

35 Y.-X. Zeng, K. Somasundaram and W. S. El-Deiry, *Nat. Genet.*, 1997, **15**, 78–82.